Diagrammatic Formulation of the Kinetic Theory of Fluctuations in Equilibrium Classical Fluids. III. Cluster Analysis of the Renormalized Interactions and a Second Diagrammatic Representation of the Correlation Functions

Hans C. Andersen

Department of Chemistry, Stanford University, Stanford, California 94305-5080

Received: March 24, 2003

This is the third of a series of papers that presents a kinetic theory of fluctuations in equilibrium classical fluids that makes extensive use of diagrammatic techniques in its development and that will facilitate the use of diagrammatic techniques in the derivation of approximate kinetic theories. The fundamental fluctuating quantity in the theory is $f(\mathbf{R},\mathbf{P})$, the density of particles (atoms) at points in single particle phase space, and the time correlation functions for fluctuations of this quantity from its average are the quantities that the theory is designed to calculate. In this paper, we start with graphical diagrammatic expressions for the correlation functions and for closely related response functions, developed in paper II, and analyze the cluster properties of the various renormalized interactions that appear in the theory. This allows us to derive a second diagrammatic formulation that has many similarities to the Mayer cluster theory for equilibrium correlation function. This second formulation allows us to express the correlation functions, response functions, and various memory functions in a common graphical language that facilitates the derivation of nonlinear relationships between, for example, the memory function and the correlation function. Such relationships are time dependent analogues of the various closures (PY, HNC, RHNC, etc.) used to obtain theories of the equilibrium structure of fluids and are central to various versions of the mode coupling theory of relaxation in fluids.

1. Introduction

The previous papers in this series,[1,2] which we shall refer to as I and II, presented a graphical formulation of the kinetic theory of fluctuations in liquids. The specific system considered was an atomic fluid, and the object of the theory is to calculate time correlation functions for fluctuations of $f(\mathbf{R},\mathbf{P}, t)$, the density of atoms in single particle phase space. The simplest of these correlation functions is

$$C(\mathbf{R}_1\mathbf{P}_1t_1;\mathbf{R}_2\mathbf{P}_2t_2) \equiv \langle \delta f(\mathbf{R}_1\mathbf{P}_1t_1)\delta f(\mathbf{R}_2\mathbf{P}_2t_2)\rangle$$

where δf is the deviation of f from its ensemble average, and the angular brackets denote an average over an equilibrium ensemble. Using the insights of Gross,[3−5] Boley,[6] and Lindenfeld,[7] we constructed a basis set, called the "fluctuation basis", for the Hilbert space of classical dynamical variables of the system and derived a linear field theory that describes the dynamics of the density fluctuations. Paper I proved various properties of the basis functions, including their existence and the cluster properties of various functions closely related to the basis. Paper II derived the equations of motion of the field theory and used the solution to express the correlation functions, as well as some closely related response functions, in diagrammatic terms. Paper II established the relationship between the present theory and that of Mazenko.[8,9] Like Mazenko's theory, the present theory can be expressed in "fully renormalized" form, which means that the vertices of the field theory that determine the dynamics of the density fluctuations can be expressed in terms of the equilibrium (static) correlations of the fluid with no reference to the interatomic potential.

The present theory, up to this point, is essentially a rederivation of the basic results of Mazenko's theory, together with a detailed justification of some of the assumptions that must be made in the derivation of the theory, such as the properties of various inverse functions (which we denoted K_n) for arbitrary values of n and diagrammatic representations of the various functions that appear in the theory.

The diagrams themselves are not directly useful for developing practical approximations. Their simple unbranched structure is a reflection of the linearity of the underlying field theory. This same linearity is the basic structure of Mazenko's theory, which has a hierarchy of correlation functions, their memory functions, memory functions of the memory functions, etc., which are linearly related.

This diagrammatic representation does, however, allows us to analyze the response functions and correlation functions in more detail than is convenient using Mazenko's notation. In this paper, we carry out such an analysis by first analyzing the cluster properties of the Q vertices, which are the renormalized interactions in the theory. This will enable us to develop a different diagrammatic representation of the various functions in the theory, one that has much in common with the Mayer cluster theory for equilibrium fluids.[10−14]

Section 2 performs the cluster analysis of the Q vertices. Section 3 derives the second diagrammatic formulation. Section 4 presents some of the immediate consequences of the formulation.

2. Cluster Analysis of the Renormalized Interactions

In the theory derived in II, the interactions responsible for the dynamics of the fluctuations are expressed by the functions $Q_{nm}(1 \ldots n; 1' \ldots m')$. These are time-independent renormalized interactions that appear in the equations of motion in eq II(4).

10.1021/jp034754m CCC: $25.00
Published on Web 08/23/2003

(An equation number preceded by I or II indicates an equation in a previous paper in this series.) An explicit formula for the functions in terms of matrix elements of the Liouville operator is given in eq II(5). As in I and II, a number, such as 1, is a "point variable" that refers to a point in single-particle phase space, such as $(\mathbf{R}_1,\mathbf{P}_1)$.

An important characteristic of such multipoint functions is their cluster properties, i.e., their behavior when one or more of the point variable arguments is well separated from the others in position space. Appendix A presents a cluster analysis of the Q_{nm} functions. It defines a set of cluster functions $Q^{(c)}_{nm}(1 \ldots n;1' \ldots m')$ for $n \geq 1$, $m \geq 1$, and $|n - m| \leq 1$. These functions have the cluster property; namely, they go to zero when one or more of the position arguments is very far from the others. Moreover, $Q^{(c)}_{n,n+1} = 0$ for $n \geq 2$. They are related to the Q_{nm} functions in a way that is most conveniently stated in terms of diagrams[15]

$$Q_{nm}(1 \ldots n; 1' \ldots m') = \text{the sum of all topologically different matrix diagrams} \quad (1)$$

with (*i*.) n left roots labeled $1 \ldots n$; (*ii*.) m right roots labeled $1' \ldots m'$; (*iii*.) one $Q^{(c)}$ vertex and δ vertices.

Here the δ vertex is associated with a function that is a Dirac delta function for two point variables; $\delta(1;1') = \delta(\mathbf{R}_1 - \mathbf{R}_{1'})\delta(\mathbf{P}_1 - \mathbf{P}_{1'})$.

The meaning of this result can be illustrated with an example

$$Q_{11}(1;1') = Q^{(c)}_{11}(1;1')$$

$$Q_{22}(12;1'2') = Q^{(c)}_{11}(1;1')\delta(2, 2') + Q^{(c)}_{11}(1;2')\delta(2, 1') + Q^{(c)}_{11}(2;1')\delta(1, 2') + Q^{(c)}_{11}(2;2')\delta(1, 1') + Q^{(c)}_{22}(12;1'2')$$

Using the idea that time proceeds from right to left, which is characteristic of the diagrammatic theory in II, we can interpret these equations in the following way. The first implies that when a fluctuation at $1'$ undergoes an interaction and forms a fluctuation at 1 the two positions must be close together. The second says that when two fluctuations at $1'$ and $2'$ undergo an interaction to form two fluctuations at 1 and 2 there are two qualitatively different things that can happen. One possibility is that one of the incoming fluctuations produces one of the outgoing fluctuations, with the other incoming fluctuation not being affected. This can happen regardless of the distance between the incoming fluctuations, and this process is described by the same $Q^{(c)}$ function as appears in Q_{11}. The second possibility, which can happen only if the two incoming fluctuations are close together, is that both incoming fluctuations together produce the two outgoing fluctuations, and the two outgoing fluctuations must be located near the positions of the incoming fluctuations.

3. Second Graphical Formulation

The fundamental dynamical quantity in the theory presented in I is $\chi(a_1;a_2)$, which is a causal response function (or propagator) defined in eq II(12). Here each a_i represents both a set of points in single-particle phase space and a time, and the response function describes how a correlated fluctuation at a_1 is affected by a change in the correlated fluctuation at a_2. The function $\chi^{(0)}(a_1;a_2)$, defined in eq II(9) is an unperturbed version of this response function.

To make diagrammatic use of the cluster expansion of the Q vertices, it is helpful to perform a complete decomposition of

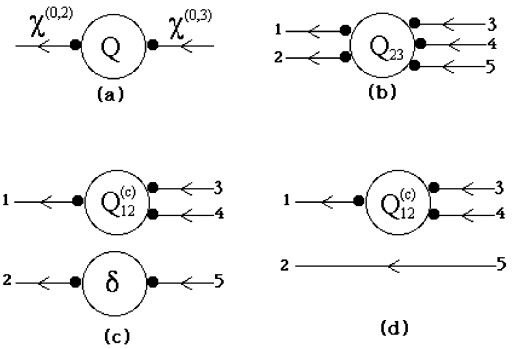

Figure 1. Informal discussion of the basic idea of the conversion from the first diagrammatic representation to the second representation. Consider a fragment of a diagram in eq 3 that has a Q vertex with a $\chi^{(0,2)}$ bond on the left and a $\chi^{(0,3)}$ bond on the right. This is depicted in part a in the upper left. When this is evaluated, the Q vertex is replaced by Q_{23} because of the fluctuation indices on the bonds. When the diagram is evaluated, α variables will be assigned to the free points. Suppose the α for the left free point is $(2; \mathbf{R}_1\mathbf{P}_1\mathbf{R}_2\mathbf{P}_2) = (2; 12)$ and the α for the right free point is $(3; \mathbf{R}_3\mathbf{P}_3\mathbf{R}_4\mathbf{P}_4\mathbf{R}_5\mathbf{P}_5) = (3; 345)$. Suppose we draw a separate line for each of the phase point variables. Then we get the diagrammatic fragment in part b in the upper right. Suppose we introduce the cluster representation of the Q_{23} as given in eq 1. One of the terms in $Q_{23}(12;345)$ is $Q^{(c)}_{12}(1;34)\delta(25)$. This term leads to a fragment that can be represented as in part c. The δ vertex demands that $(\mathbf{R}_2\mathbf{P}_2) = (\mathbf{R}_5\mathbf{P}_5)$ so we might as well just have a single line labeled $(\mathbf{R}_2\mathbf{P}_2) = 5$ extending across this segment of the diagram, in recognition of the fact that this term in the cluster expansion of Q_{23} has no effect on the fluctuation labeled 5. See Appendix B for a more systematic and rigorous discussion.

$\chi^{(0)}$ along the lines suggested by eq II(16)

$$\chi^{(0)}(a;a') = \sum_{p=0}^{\infty} \chi^{(0,p)}(a, a')$$

where

$$\chi^{(0,p)}(a, a') = \delta_{n(a),p}\chi^{(0)}(a;a') \quad (2)$$

$\chi^{(0,p)}$ is an unperturbed propagator for a set of p correlated fluctuations. When this is substituted into eq II(13), the following graphical expression for χ is obtained:

$$\chi(a_1;a_2) = \text{the sum of all topologically different connected matrix diagrams} \quad (3)$$

with (i) a left root labeled a_1; (ii) a right root labeled a_2; (iii) free points; (iv) $\chi^{(0,p)}$ bonds for $p \geq 1$; and (v) Q vertices, such that (i) each root is attached to a $\chi^{(0,p)}$ bond and (ii) each free point is attached to a $\chi^{(0,p)}$ bond and a Q vertex.

The diagrams in this series look exactly like the diagrams in Figure 1 of II provided the lines in that figure are interpreted as $\chi^{(0,p)}$ bonds rather than $\chi^{(0)}$ bonds. Each diagram in eq II(13) is a sum of one or more of the diagrams in this series.

In every nonzero diagram in this series, each $\chi^{(0,p)}$ bond is attached to free points on two different Q hypervertices. When a diagram is evaluated, a set of $\mathbf{R}^p\mathbf{P}^p$ integration variables is attached to each free point at each end of each $\chi^{(0,p)}$. However, $\chi^{(0,p)}$ contains delta functions that demand that the integration variables associated with each of its ends be the same and that the fluctuation index for each must be p. [See eqs II(9) and 2.] In effect, therefore, each $\chi^{(0,p)}$ bond has associated with it a single set of $\mathbf{R}^p\mathbf{P}^p$ variables. In drawing the diagrams, we could replace the single line for $\chi^{(0,p)}$ by p lines and put one phase point variable on each of the lines. Compare parts a and b of Figure

1. The p new lines would represent unperturbed propagation of p individual fluctuations, whereas the original single line represented unperturbed propagation of a set of p fluctuations.

Now we introduce the cluster expansion of the Q vertices into the series, leading to diagrams in which a $Q^{(c)}$ vertex and zero or more δ vertices (together with some additional complications, which are addressed in Appendix B) replace each of the original Q vertices. Compare parts b and c of Figure 1. If one of the p lines of a $\chi^{(0,p)}$ is attached to a δ vertex rather than the $Q^{(c)}$ vertex, it is in an important sense not involved in or affected by the interaction that the $Q^{(c)}$ represents; moreover, it has a δ function connection to another point, which in turn has a line attached. One can imagine that the uninvolved fluctuation could be represented by a line that "goes right by" the $Q^{(c)}$. Compare parts c and d of Figure 1. The kinds of pictures that are generated by the combination of the cluster representation of the Q and the decomposition of $\chi^{(0)}$ suggests a new diagrammatic representation in which lines represent individual fluctuations that interact only at $Q^{(c)}$ vertices.

A detailed analysis of the conversion of the series into a form containing this new type of diagram is presented in Appendix B. The considerations are rather detailed, but the final results are (in comparison) rather simple. In the new series, each diagram contains points, and each point has associated with it a single phase point variable and a time. The diagrams also contain $Q^{(c)}_{mn}$ vertices and $\chi^{(0)}$ lines. A $Q^{(c)}_{mn}$ vertex represents a function

$$Q^{(c)}_{mn}(1t_1 \ldots mt_m; 1't_{1'} \ldots n't_{n'}) = Q^{(c)}(1 \ldots m; 1' \ldots m') \left(\prod_{i=2}^{m} \delta(t_1 - t_i)\right)\left(\prod_{j=1}^{n} \delta(t_1 - t_{j'})\right)$$

and a $\chi^{(0)}$ line represents a function

$$\chi^{(0)}(1t_1; 1't_{1'}) = \Theta(t_1 - t_1')\delta(1, 1') \tag{4}$$

The new graphical expression for the response function is

$$\chi_{\mathrm{nm}}(1 \ldots n, t; 1' \ldots m', t') = \text{the sum of all topologically different matrix diagrams} \tag{5}$$

with (i) n left roots labeled (1, t), (2, t), ..., (n, t); (ii) m right roots labeled (1′, t'), (2′, t'), ..., (m', t'); (iii) free points; (iv) $\chi^{(0)}$ bonds; and (v) $Q^{(c)}$ vertices; such that (i) each root is attached to a $\chi^{(0)}$ bond and (ii) each free point is attached to a $\chi^{(0)}$ bond and a $Q^{(c)}$ vertex.

See Figure 2 for some examples of the diagrams for χ_{11} and Figure 3 for some diagrams for χ_{22}. These diagrams have symmetry numbers that differ from unity. See Appendix A of I for a brief discussion of symmetry numbers.

The correlation function $C_{nm}(1 \ldots nt; 1' \ldots m', 0)$, defined in eq II(14), describes the correlations among a set of n fluctuations at one time and a set of m fluctuations at a different time. It can be calculated from a response function using eq II(15). That equation can be given a simple diagrammatic meaning in terms of these new types of diagrams because of the presence of the $1/m!$ factor, which can be regarded as the symmetry number of a diagram

$$C_{nm}(1 \ldots n, t_1; 1' \ldots m', 0) = \text{one matrix diagram} \tag{6}$$

with (i) n left roots labeled (1, t_1),(2, t_1), ..., (n, t_1); (ii) m right roots labeled (1′, 0), (2′, 0), ..., (m', 0); (iii) m free points; (iv) one χ_{nm} vertex and one F_m vertex; such that (i) every left root is a left point of the χ_{nm}; (ii) every right root is a right point of the F_{m}; and (iii) every free point is on both a χ_{nm} and the F_{m}.

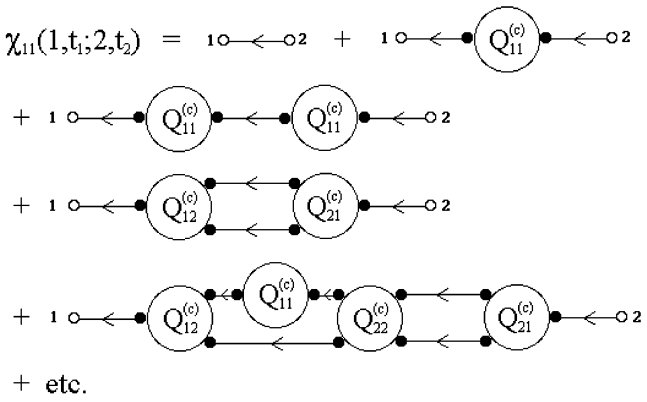

Figure 2. Graphical series for $\chi_{11}(1, t_1;2, t_2)$ according to eq 3. This is the second diagrammatic formulation. In each diagram, the left root should be labeled with (1, t_1) and the right root with (2, t_2), but we have omitted the time variable for simplicity. Each line with an arrow is a $\chi^{(0)}$ bond. See eq 4. Each large circle is a $Q^{(c)}_{nm}$ vertex. These are all matrix diagrams in the sense defined in Appendix A of I. Each $Q^{(c)}$ is drawn so that the points on the left correspond to the left arguments of its function and the points on the right correspond to the right arguments. Each line is drawn horizontally with the arrow pointing to the left, and the point at the left (right) end corresponds to the left (right) argument of the function. Each free point (filled circle) has two things attached (a vertex and a line), and each root point (small open circle) has one thing attached (a line).

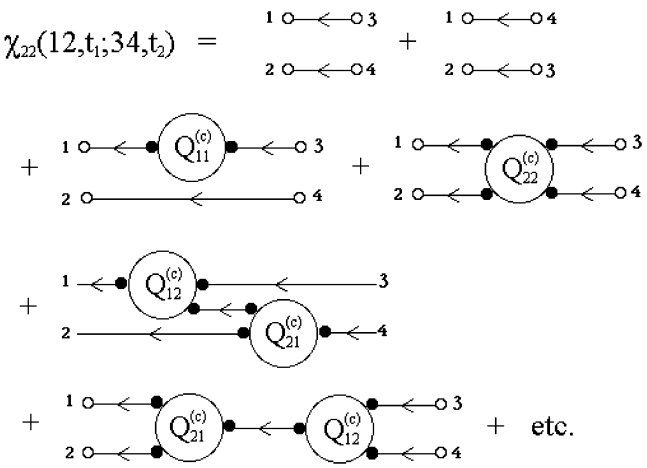

Figure 3. Graphical series for $\chi_{22}(1, t_1;2, t_2)$ according to eq 3. This is the second diagrammatic formulation. In each diagram, the left roots should be labeled with (1, t_1) and (2, t_1) and the right roots with (3, t_2) and (4, t_2), but we have omitted the time variables for simplicity. See the caption of Figure 2 for additional information.

(For future reference we note that the special case of this for C_{11} is

$$C_{11}(1, t_1;1', 0) = \int \mathrm{d}1'' \, \chi_{11}(1, t_1; 1'', 0)F_1(1''; 1')$$

which leads to

$$\chi_{11}(1, t_1; 1', 0) = \int \mathrm{d}1'' \, C_{11}(1, t_1; 1'', 0)K_1(1''; 1') \tag{7}$$

when the inverse relationship, eq I(13) between K_1 and F_1 is used.)

Equations 5 and 6 are the major new results of this paper. They represent formally exact diagrammatic expressions for the time correlation functions of the fields defined using the

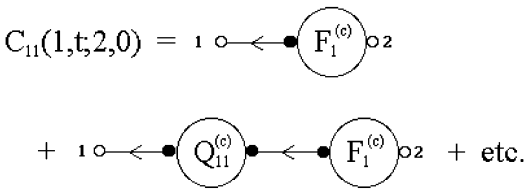

Figure 4. Graphical series for the correlation function $C_{11}(1, t;2, 0)$ in the second diagrammatic formulation. In each diagram, the left root should be labeled (1, *t*) and the right root should be labeled (2, 0), but we have omitted the time variables for simplicity. The vertex at the right of each diagram is an $F_1^{(c)}$ vertex. See the caption of Figure 2 for additional information. The general diagram in this series can be obtained from the general diagram in Figure 2 for $\chi_{11}(1, t_1;2, t_2)$ by attaching left point of an $F_1^{(c)}$ to the right root of the diagram, changing the right root to a free point, and putting a root point on the right of the $F_1^{(c)}$.

fluctuation basis and for the response functions associated with the fields. Because the correlation functions of the fluctuation basis fields are directly related to those for the phase space densities, we have a complete formal diagrammatic theory for all of the two time correlation functions of the phase space densities.

Having both of the functions and response functions in the same diagrammatic language facilitates theoretical manipulations involving them. For example, using the generalization of some theorems of Morita and Hiroike, we can substitute the graphical expression eq 5 for χ into that for C to get a more detailed expression for C

$$C_{nm}(1 \ldots n, t_1; 1' \ldots m', 0) = \text{the set of all topologically different matrix diagrams} \quad (8)$$

with (i) n left roots labeled $(1, t_1)$, $(2, t_1)$, ..., (n, t_n); (ii) m right roots labeled $(1', 0)$,$(2', 0)$, ..., $(m', 0)$; (iii) free points; (iv) χ_0 bonds; and (v) $Q^{(c)}$ vertices and one F_n vertex; such that (i) each left root is attached to a $\chi^{(0)}$ bond; (ii) each right root is attached to an F_n vertex; and (iii) each free point is attached to a $\chi^{(0)}$ bond and either a $Q^{(c)}$ or the F_n.

See Figure 4 for some of the diagrams in this series for the case of C_{11}.

4. Consequences

In this section, we shall state some consequences that follow almost immediately from the new graphical formulation.

4.1. Cluster Properties of the Response Function. The diagrams in eq 5 for χ_{nm} need not be connected. However, each connected diagram is a function of its arguments that is zero if any one or more of the arguments is far from from all of the others; that is, it has the cluster property. This follows because both the $Q^{(c)}$ vertices and the $\chi^{(0)}$ bonds have this property. Accordingly we define

$$\chi_{nm}^{(c)}(1 \ldots n, t; 1' \ldots m', t') \equiv \text{the sum of all connected diagrams in eq 5 for } \chi_{nm}(1 \ldots n, t; 1' \ldots m', t') \quad (9)$$

It follows from the previous discussion that $\chi_{nm}^{(c)}$ has the cluster property.

The χ function can be expressed in terms of the $\chi^{(c)}$ functions. We find

$$\chi_{nm}(1 \ldots n, t; 1' \ldots m', t') = \text{the sum of all topologically different matrix diagrams} \quad (10)$$

with (i) n left roots labeled $(1, t)$, $(2, t)$, ..., (n, t); (ii) m right roots labeled $(1', t')$,$(2', t')$, ..., (m', t'); and (iii) $\chi_{pq}^{(c)}$ vertices for $p, q \geq 1$.

4.2. Cluster Properties of the Correlation Functions. The static correlation functions F_n have cluster properties that are conveniently expressed in terms of cluster functions $F_n^{(c)}$. See eq I(3.7). These cluster functions have the cluster property. Substituting eqs 10 and I(20) into eq 8 we get

$$C_{nm}(1 \ldots n, t; 1' \ldots m', 0)\rangle = \text{the sum of all topologically different matrix diagrams} \quad (11)$$

with (i) n left roots labeled $(1, t)$,$(2, t)$, ..., (n, t); (ii) m right roots labeled $(1', 0)$, $(2', 0)$, ..., $m', 0)$; (iii) free points; and (iv) $\chi_{pq}^{(c)}$ vertices for $p, q \geq 1$ and $F_p^{(c)}$ vertices for $p \geq 1$; such that (i) each left root is attached to a $\chi_{pq}^{(c)}$; (ii) each right root is attached to an $F_p^{(c)}$; and (iii) each free point is attached to a right point of a $\chi_{pq}^{(c)}$ and a left point of an $F_p^{(c)}$ and nothing else.

The cluster functions for C are defined as

$$C_{nm}^{(c)}(1 \ldots n, t; 1' \ldots m', 0) = \text{the sum of the connected diagrams in eq 11 for } C_{nm}(1 \ldots n, t; 1' \ldots m', 0)$$

Each of these cluster functions has the cluster property. Then

$$C_{nm}(1 \ldots n, t; 1' \ldots m', 0) = \text{the sum of all topologically different diagrams}$$

with (i) n left roots labeled $(1, t)$, $(2, t)$, ..., (n, t); (ii) m right roots labeled $(1', 0)$, $(2', 0)$, ..., $(m', 0)$; and (iii) $C_{pq}^{(c)}$ vertices for $p, q \geq 1$.

4.3. Diagrammatic Series for the Collisional Part of the Memory Function. The collisional part of the memory function for the usual kinetic equation for the correlation function of single-point fluctuations is given in eq II(23) in terms of the function $\chi_{22}^{(>1)}$. This function is defined in eq II(22) as the sum of diagrams in the series for χ_{22} that have no $\chi^{(0,1)}$ bonds. Diagrams of the original series for χ that have $\chi^{(0,1)}$ bonds lead to diagrams in the new series for χ that have $\chi^{(0)}$ bonds (now describing single point fluctuations) such that removal of just one bond disconnects both left roots from both right roots. It follows that

$$\chi_{22}^{(>1)}(12, t; 1'2', t') = \text{the sum of all the diagrams}$$

in eq 5 for $\chi_{22}(12, t; 1'2', t')$ that have no $\chi^{(0)}$ bond whose removal disconnects the left roots from the right roots.[16]

We can now provide a diagrammatic formula for M, the collisional part of the memory function in the kinetic equation for the single-point fluctuation correlation function

$$M(1, t_1;2, t_2) = \text{the sum of all topologically different connected matrix diagrams} \quad (12)$$

with (i) a left root labeled $(1, t_1)$; (ii) a right root labeled $(2, t_2)$; (iii) free points; (iv) $Q^{(c)}$ vertices; and (v) $\chi^{(0)}$ bonds; such that (i) the left root is attached to a $Q_{12}^{(c)}$ vertex; (ii) the right root is attached to a $Q_{21}^{(c)}$ vertex; (iii) every free point is attached to a $\chi^{(0)}$ bond and a $Q^{(c)}$ vertex; and (iv) there is no $\chi^{(0)}$ bond whose removal disconnects the two roots.

See Figure 5 for examples of these diagrams.

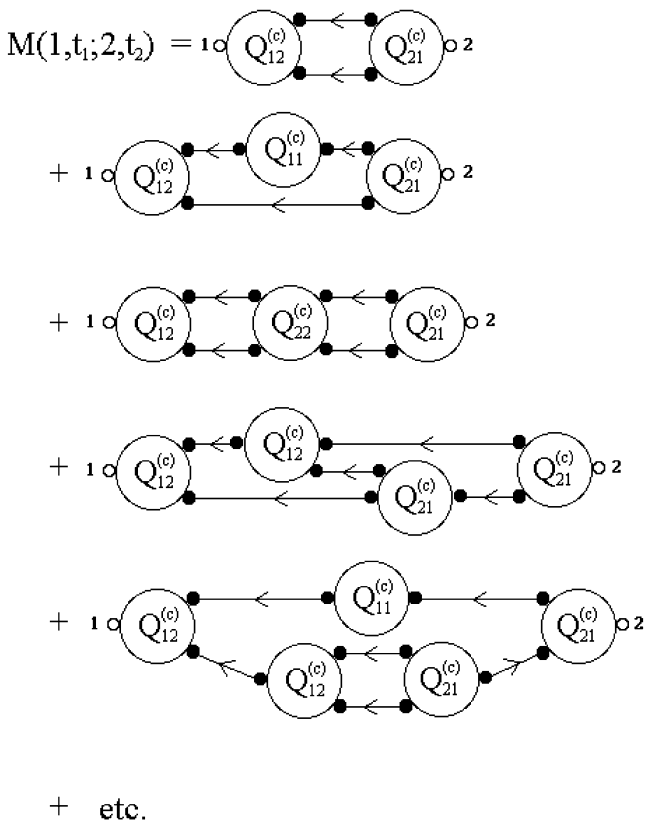

Figure 5. Graphical series for the collisional part of the memory function of the phase space density fluctuation correlation function. See the text for a discussion of how the formally exact series can be used to derive a simple mode coupling approximation. Note that some diagrams have the property that if the left and right $Q^{(c)}$ vertices are removed the diagram become disconnected into two pieces. Each of the pieces looks like a member of the series for χ_{11} (with the root points removed). See Figure 2. The sum of all such diagrams is equal to a single diagram that looks like the first diagram here with each of the $\chi^{(0)}$ bonds replaced by a χ_{11} vertex.

4.4. Derivation of Closure Relations. An important feature of the second diagrammatic representation we have developed is that the memory function and the correlation functions are each expressed exactly in terms of diagrams that are closely related in structure. This may facilitate the derivation of closure relationships between the memory function and the correlation function.

To illustrate how this might be done using these diagrams, we shall "derive" a particularly simple approximation that is of the form of a "simple mode coupling theory" approximation, as defined by the theory of Götze and co-workers.[17] The approximation we will derive is probably not an accurate one, but it will allow us to discuss how more accurate mode coupling approximations might be derived.

The series for the memory function is given in eq 12 and Figure 5. Note that some of the diagrams in the series become disconnected if the $Q^{(c)}$ vertices on the far left and far right are removed, whereas others remain connected. Suppose we were to choose to approximate M by the subset of diagrams that become disconnected when these two vertices are removed. In each such diagram, each of the two pieces that becomes disconnected is in the series for χ_{11}. See Figure 2. Using basic diagrammatic arguments, it is straightforward to show that the sum of all such diagrams is a single diagram that looks like the first diagram in Figure 5 with each $\chi^{(0)}$ vertex replaced by a χ_{11} vertex. This approximation then gives the following result:

$$M(1, t_1; 2, t_2) = \frac{1}{(2!)^2}\int \mathrm{d3\ d4\ d5\ d6}\ Q_{12}(1; 34) \times \chi_{11}(3, t_1; 5, t_2)\chi_{11}(4, t_1; 6, t_2)Q_{21}(56; 2)$$

Using eq 7, each of the response functions can be expressed in terms of the corresponding correlation function

$$M(1, t_1;2, 0) = \frac{1}{(2!)^2}\int \mathrm{d3\ d4\ d5\ d6}\ Q_{12}(1; 34) \times \int \mathrm{d7}\ C_{11}(3, t_1; 7, 0)K_1(7; 5) \times \int \mathrm{d8}\ C_{11}(4, t_1; 8, 0)K_1(8, 6)Q_{21}(56; 2)$$

This result is of the form of a "simplified mode coupling theory" approximation. It expresses the memory function for a specific time as a quadratic function of the correlation function at the same time.

This procedure shows how mode coupling approximations can be derived by identifying regions of the diagrams in the series for the memory function that have the characteristic that two (or more) single-point fluctuations are propagating independently with no connection between them. The values associated with those regions look like products of χ_{11} response functions, which can then be related to products of correlation functions. This particular version of a simplified mode coupling approximation is probably too simple to be accurate, in that on each side of the region of independent propagation we have simply a single renormalized interaction. For an accurate mode coupling approximation, the quantity on each side of the region of independent propagation should probably be a classical T matrix element for a binary collision. In addition, there should be a term that describes a simple completed binary collision in the absence of mode coupling effects. Ideas of this type have been used by Mazenko[9] and by Sjögren,[18] and we plan to explore them in the context of the present graphical theory.

5. Discussion

In this series of papers, we have presented a formally exact diagrammatic theory of the two time correlation functions of phase space density fluctuations in an atomic fluid at equilibrium. In this paper, we have shown that the correlation functions for density fluctuations, as well as associated response functions and the memory function, can be expressed in terms of diagrammatic series, as in Figures 2−5, that have much in common with the Mayer cluster series[10−14] for static correlation functions of an equilibrium fluid. Each point in the new series corresponds to a position, a momentum, and a time variable, whereas in Mayer's theory, each point corresponds to a position. The interactions in the new series are represented by $Q^{(c)}$ vertices, which contain the physics of the two-particle potential but are fully renormalized, in the sense that they can be expressed in terms of the static correlation functions with no reference to the potential. The new series also contains vertices corresponding to the initial values of the correlation functions, as well as a very simple unperturbed causal response function.

An important feature of the theory is that the same types of diagrams are used to express both the correlation functions and the memory functions, as well as the closely related response functions. This is analogous to the situation in Mayer's cluster theory of equilibrium liquids, namely, that correlation functions and direct correlation functions are described using the same types of diagrams, thus facilitating the derivation of various closures for the Ornstein−Zernike equation. The use of such

relationships is central to the various versions of mode coupling theory, and the present diagrammatic theory may be useful for deriving mode coupling theories and corrections to such theories, while still keeping track of all the contributions to the formally exact answer.

Acknowledgment. This work was supported by the National Science Foundation through grants CHE-9734893 and CHE-0010117. I thank Dr. Steven Pitts for very helpful conversations.

A. Cluster Properties of the *Q* Functions

The cluster properties of the Q functions are consequences of the cluster properties of the J, F, and K functions defined in I and of matrix elements of the Liouville operator, whose calculation is discussed in Appendix A of II. Derivation of the result is a straightforward (but tedious) exercise in the use of graphical techniques developed in I and II. Here we shall outline the derivation of the cluster properties rather than present the argument in detail.

The original formula for the Q functions is eq II(5), which we rewrite as

$$-Q_{nm}(1 \ldots n; 1' \ldots m') = \frac{1}{m!}\int \mathrm{d}1'' \ldots \mathrm{d}m'' \langle \phi_n(1 \ldots n)|iL|\phi_m(1'' \ldots m'')\rangle \times K_m(1'' \ldots m''; 1' \ldots m') \quad (13)$$

We have used the symmetry of K_m under interchange of its left and right arguments. Also, the Hermitian character of L implies that

$$\langle \phi_n|L|\phi_m\rangle = -\langle \phi_m|L|\phi_n\rangle \quad (14)$$

because this matrix element is purely imaginary.

A.1. $Q_{n,n+1}$. Applying eq 13 to the calculation of $Q_{n,n+1}$ and using eqs II(A2) and I(2.13), we find that

$$Q_{n,n+1}(1 \ldots n; 1' \ldots (n+1)') = \text{the set of all topologically different diagrams} \quad (15)$$

with (i) n left roots labeled $1 \ldots n$; (ii) $n+1$ right roots labeled $1' \ldots (n+1)'$; and (iii) one V_{12} vertex and δ vertices.

This verifies eq 2 for $m = n + 1$ and gives the following result:

$$Q^{(c)}_{12}(1; 1'2') = V_{12}(1; 1'2')$$

$$Q^{(c)}_{n,n+1} = 0 \text{ for } n \geq 2$$

Note that $Q^{(c)}_{12}$ has the cluster property if the potential is shortranged.

A.2. $Q_{n,n-1}$. Applying the same equations to the calculation of $Q_{n,n-1}$ leads to a result that can converted to diagrammatic language

$$-Q_{n,n-1}(1 \ldots n; 1' \ldots (n-1)') = \text{the matrix diagram} \quad (16)$$

with (i) n left roots labeled $1 \ldots n$; (ii) $n-1$ right roots labeled $1' \ldots (n-1)'$; (iii) $n+2$ free points; and (iv) one F_n vertex, one V^T_{21} vertex, and one K_{n-1} vertex; such that (i) the left roots are on the F_n; (ii) the right roots are on the K_{n-1}; (iii) two free points are right points on the F_n and left points on the V^T_{21}; (iv) $n-2$ free point are right points on the F_n and left points on the K_{n-1}; and (v) one free point is the right point on the V^T_{21} and a left point of the K_{n-1}.

(Here the V^T_{21} function is defined as $V^T_{21}(12;1') \equiv V_{12}(1';12)$.) Introduce the cluster expansion, eqs I(3.7) and I(3.8), of the F_n and K_{n-1} in terms of $F^{(c)}$ and $K^{(c)}$ vertices. Some diagrams are completely connected, and their sum is defined as $-Q^{(c)}_{n,n-1}$. (This implies that $Q^{(c)}_{n,n-1}$ has the cluster property.) Others are disconnected. In a disconnected diagram, a subgraph that does not contain the V^T_{21} might contain just one $F^{(c)}_1$ and one $K^{(c)}_1$, or it might be more complicated. It is straightforward to show, using eq I(B4), that the sum of the diagrams with more complicated subgraphs is zero. The remaining disconnected graphs sum to a result that is of the form of the disconnected diagrams in eq 1 for $m = n - 1$.

A.3. Q_{nn}. The matrix element of the Liouville operator that is needed is $\langle \phi_n|iL|\phi_n\rangle$. Using eq I(7) for the second ϕ_n gives the following exact result:

$$\langle \phi_n|iL|\phi_n\rangle = \langle \phi_n|iL(1 - P_{n-1})|\psi_n\rangle \quad (17)$$

because the subsequent terms in the series for ϕ_n are in subspaces that are orthogonal to the ϕ_n on the left side of this inner product. We used eq I(10) for the projection operator and eq II(26) for the calculation of the Liouville operator matrix elements. In particular

$$\langle \phi_n(1 \ldots n)|iL|\psi_n(1'' \ldots n'')\rangle = \sum_{i''=1}^{n}\int \mathrm{d}1''' F_n(1 \ldots n; 1'' \ldots n''[1'''/i''])V^T_{11}(1'''; i'') + \sum_{i''=1}^{n}\int \mathrm{d}1''' \mathrm{d}2''' J_{n,n+1}(1 \ldots n; 1'' \ldots n''2'''[1'''/i'']) \times V^T_{21}(1'''2'''; i'')$$

(See eq II(3) for a discussion of the meaning of the notation using square brackets.) We then substitute this expression into eq (13) for Q_{nn}. The result can be expressed as three sums of diagrams. The first sum contains V^T_{11} and is derived from the 1 term in (17). The second sum contains V^T_{21} and is derived from the 1 term in (17). The third sum contains V^T_{21} and is derived from the P term in (17). We then replace each K, J, and F by its cluster expansion in terms of $K^{(c)}$, $J^{(c)}$, and $F^{(c)}$, in each of these three sums.

By a procedure very similar to that described above for $Q_{n,n-1}$, it is straightforward to show that the first sum has the structure of eq 2. The completely connected diagrams in the sum are contributions to $Q^{(c)}_{n,n-1}$, and the disconnected diagrams are a sum of products of a $Q_{m,m-1}$ for $m < n$ and of delta functions.

In the second and third sums, it is straightforward to show that each nonzero diagram has one $J^{(c)}$ vertex with a different number of left points than right points and one V^T_{21} that has two left points and one right point and that all other vertices have equal numbers of left and right points. (Note than any $J^{(c)}$ vertex with equal numbers of left and right points is equivalent to an $F^{(c)}$ vertex.)

In the second and third sums, some diagrams are connected, and the sum of all of these is a contribution to $Q^{(c)}_{n,n-1}$. In some of the disconnected diagrams, the $V^{(c)}_{21}$ and the $J^{(c)}$ with different numbers of left points and right points are in different subgraphs. It can be shown that these diagrams cancel between the two sums because of the difference of sign of the two sums. In the remaining disconnected diagrams, the $V^{(c)}_{21}$ and the $J^{(c)}$ with different numbers of left points and right points are in the same subgraph. In some of these diagrams all of the other

subgraphs contain only $F_1^{(c)}$ and $K_1^{(c)}$ vertices and are equivalent to delta functions. In others of the diagrams, one or more of the other subgraphs contains $F_m^{(c)}$ and/or $K_m^{(c)}$ vertices with $m > 1$. The sum of all of these diagrams can be shown to be zero, using eq I(25).

The net result is that, when the diagrams that systematically cancel one another are removed from the series, every remaining diagram has: one connected subgraph containing one V^T vertex (as well as one or more F_m, one or more K_m, and, in the case that the V^T is a V_{21}^T, one $J^{(c)}$ with unequal numbers of left and right points) and zero or more subgraphs that are delta functions each having one left root and one right root attached. The result leads to eq 1. The $Q_{nn}^{(c)}$ function is the sum of all of the connected diagrams in the final result for Q_{nn}, and therefore, it has the cluster property.

B. Derivation of Diagrammatic Series Containing Points and Lines for Individual Fluctuations

Here we derive a new diagrammatic formulation, one in which each point and line represents a fluctuation at a single-phase point rather than a collection of n fluctuations at n phase points. A complete proof would require a great deal of detailed explanation. To avoid this, we shall indicate the major steps in the logical development and mention the major considerations that justify each step.

The starting point is eq 3. To get a new diagrammatic series, we perform the following transformation of each diagram in this series:

i. Replace each old root point, labeled by $a \leftrightarrow (n, 1 \ldots n, t) \leftrightarrow (n,\mathbf{R}_1\mathbf{P}_1 \ldots \mathbf{R}_n\mathbf{P}_n, t)$, by n new root points labeled by $(1t)(2t) \ldots (nt)$ or $(\mathbf{R}_1\mathbf{P}_1t) \ldots (\mathbf{R}_n\mathbf{P}_nt)$.

ii. Replace each old free point by n new free points. The value of n is the fluctuation index associated with the old point, as determined from the vertex to which the point is attached.

iii. Replace each old Q_{nm}, having one left point and one right point, by a new Q having n left points of the new type and m right points of the new type. The function associated with the old Q depended on the α variables. The function associated with the new Q has the same dependence on the α variables but contains enough delta functions to make all the time arguments equal. That is

$$Q_{nm}(1t_1 \ldots nt_n; 1't_{1'} \ldots m't_{m'}) = Q_{nm}(1 \ldots n; 1' \ldots m')\left(\prod_{i=2}^{n}\delta(t_i - t_1)\right)\left(\prod_{j=1}^{m}\delta(t_{j'} - t_1)\right) \quad (18)$$

Here, the Q on the left is the function associated with the new Q_{nm} vertex and the Q on the right is the function associated with the old vertex.

iv. Replace each $\chi^{(0,p)}$ bond by p $\chi^{(0)}$ bonds. Each $\chi^{(0)}$ bond, like the $\chi^{(0,p)}$ bonds of the previous series, is represented by a line with an arrowhead. Each line is attached to two new points such that the head end of the new bond is attached to a new point that resulted from the point at the head end of the bond that is being replaced. A similar statement applies to the point attached to the tail of a new $\chi^{(0)}$. The function associated with a $\chi^{(0)}$ bond is

$$\chi^{(0)}(1t_1; 2t_2) \equiv \delta(1; 2)\Theta(t_1 - t_2)$$

Because each Q_{nm} is left symmetric and right symmetric and the free points are not labeled, each old diagram generates only one possible topologically distinct diagram; that is, there is only one topologically distinct way of attaching the $\chi^{(0)}$ bonds to the new free points. Moreover, different diagrams in the old series lead to topologically distinct diagrams in the new series.

When we evaluate a new diagram using the usual rules for evaluation of diagrams and the functions given above for the new $\chi^{(0)}$ bond and the new Q vertices, we find that the value of each new diagram is equal to the value of the corresponding old diagram. Proving this requires detailed consideration of the range of summation over α for each of the free points in the old diagram and of the fact that the new diagrams have symmetry numbers that are not all unity. We shall omit the details of that proof.

The result is

$\chi_{nm}(1 \ldots n, t_1; 1' \ldots m', t_2) =$ the sum of all topologically different connected matrix diagrams

with (i) n left roots labeled $(1, t_1) \ldots (n, t_1)$; (ii) m right roots labeled $(1', t_2) \ldots (m', t_2)$; (iii) free points; (iv) $\chi^{(0)}$ bonds; and (v) Q_{pq} vertices for $p, q \geq 1$; such that (i) each root is attached to a $\chi^{(0)}$ bond; (ii) every free point is attached to a $\chi^{(0)}$ bond and a Q vertex; and (iii) for diagrams with one or more Q, the head points of all $\chi^{(0)}$ bonds whose tails are attached to right roots are on the same Q, and the head points of all $\chi^{(0)}$ bonds whose tails are attached to the left points of the same Q have their heads either on the same Q or all on left roots.

In a diagram, a forward path from one point to another will be defined as a sequence of points, bonds, and vertices, starting with the first point and ending with the second point, such that each item in the sequence is attached to the next item in the sequence and for each bond in the sequence the tail point precedes the head point in the sequence.

A consequence of the stipulations in this series (excluding restriction iii) is that there is a forward path from any point to any left root. If we keep all of the other specifications the same, we can replace the restriction iii by the statement that, for diagrams with one or more Q, all forward paths from a right root to a left root contain all of the Q vertices and contain them in the same order. We get

$\chi_{nm}(1 \ldots n, t_1; 1' \ldots m', t_2) =$ the sum of all topologically different connected matrix diagrams

with (i) n left roots labeled $(1, t_1) \ldots (n, t_1)$; (ii) m right roots labeled $(1', t_2) \ldots (m', t_2)$; (iii) free points; (iv) $\chi^{(0)}$ bonds; and (v) Q_{pq} vertices for $p, q \geq 1$; such that (i) each root is attached to a $\chi^{(0)}$ bond; (ii) every free point is attached to a $\chi^{(0)}$ bond and a Q vertex; and (iii) for diagrams with one or more Q, all forward paths from a right root to a left root contain all the Q vertices and contains them in the same order.

In the diagrammatic formulation above, as in all of the preceding ones, the diagrams are in effect strictly time ordered. (By this we mean that the structure of the diagrams strictly determines the relative values of the time variables for which the integrand of the integral in the value of the diagram is nonzero. For example, for this latest series, when a diagram is evaluated, all of the times associated with the right roots are the same, all of the times associated with each Q are the same, and all the times associated with the left roots are the same. Thus, if there are r Q vertices, there are $r + 2$ distinct times. Moreover, the Heaviside time dependence of the $\chi^{(0)}$ bonds and the last topological restriction in the series implies that the integrand is nonzero only when these times are strictly ordered in the same sequence as is implied by the forward paths from a right root to a left root.) However, the diagrammatic result

that we will finally obtain in this appendix is one in which such strict time ordering is not implied by the structure of the diagrams. (It will still be the case that there will be one time for each $Q^{(c)}$, but there will be instances in which the two times associated with two $Q^{(c)}$s can be in either order.) Proving that a series of diagrams that are not strictly time ordered is equal to a series of diagrams that are strictly time ordered requires special considerations of symmetry numbers and of other topological details. Essentially, the same problem was encountered by Hugenholtz[19] in quantum many-body theory and solved for the relevant type of diagrams in the Laplace transform domain, but adaptation of that solution to the present problem would be rather complicated. Instead, we shall address the problem in such a way that generalizations of the theorems of Morita and Hiroike[11−13] can be used to carry out the derivation.

We introduce a new type of point, which we call a time point (because it has only a time argument associated with it). We associate an additional time argument with each new Q_{nm}. In the diagrams, a time point will be associated with that new argument. The function associated with this newer Q_{nm} is given by

$$Q_{nm}(1t_1 \ldots nt_n; t; 1't'_1 \ldots m't'_m) = Q_{nm}(1t_1 \ldots nt_n; 1't'_1 \ldots m't_{m'})\delta(t - t_1) \quad (19)$$

where the Q on the left is the newer Q and the Q on the right is the new Q. Making this change causes a slight change in the way a diagram is evaluated, with one additional time integration for each time point, but it does not change the value of any diagram. We extend the definition of matrix diagram (see Appendix A of I) to diagrams that have time points in the following way: a diagram with time points will be called a matrix diagram if it is a matrix diagram according to the old definition when the time points (and Θ bonds, which are defined below) are removed. Then we have

$$\chi_{nm}(1 \ldots n, t_1; 1' \ldots m', t_2) = \text{the sum of all topologically different connected matrix diagrams} \quad (20)$$

with (i) n left roots labeled $(1, t_1) \ldots (n, t_1)$; (ii) m right roots labeled $(1', t_2) \ldots (m', t_2)$; (iii) free points and free time points; (iv) $\chi^{(0)}$ bonds; and (v) Q_{pq} vertices for $p, q \geq 1$; such that (i) each root is attached to a $\chi^{(0)}$ bond; (ii) every free point is attached to a $\chi^{(0)}$ bond and a Q vertex; (iii) each free time point is attached to a different Q vertex; and (iv) for diagrams with one or more Q, all forward paths from a right root to a left root contain all the Q vertices and contain them in the same order.

Next we introduce the Θ bond, which can be be represented as a line with an arrowhead. Each end of a Θ bond can be attached either to a root or to a time point. The function associated with the Θ bond is simply a Heaviside function of the time associated with the point at the head end minus the time associated with the time at the tail end.

In a diagram, a forward path of $\chi^{(0)}$ bonds will be defined as a forward path in which all of the bonds are $\chi^{(0)}$ bonds. A forward path of Θ bonds will be defined as a forward path in which all of the bonds are Θ bonds. In the previous series, the forward paths that are mentioned are all forward paths of $\chi^{(0)}$ bonds.

In each diagram, we add Θ bonds in order to construct one forward path of Θ bonds from root $1'$ to root 1 such that the path visits the time point on each Q once and only once. This generates a new diagram. We repeat this process in all possible ways, generating several diagrams from each diagram in eq 20. If the forward path of Θ bonds visits the Q vertices in the same order as the forward path of $\chi^{(0)}$ bonds, the value of the diagram is unchanged by this. If the forward path visits the Q vertices in a different order, the value of the diagram is zero, so there is no error made by including the diagram in the series. We have

$$\chi_{nm}(1 \ldots n, t_1; 1' \ldots m', t_2) = \text{the sum of all topologically different connected matrix diagrams} \quad (21)$$

with (i) n left roots labeled $(1, t_1) \ldots (n, t_1)$; (ii) m right roots labeled $(1', t_2) \ldots (m', t_2)$; (iii) free points and free time points; (iv) $\chi^{(0)}$ and Θ bonds; and (v) Q_{pq} vertices for $p, q \geq 1$; such that (i) each root is attached to a $\chi^{(0)}$ bond; (ii) every free point is attached to a $\chi^{(0)}$ bond and a Q vertex; (iii) for diagrams with one or more Q, all forward paths of $\chi^{(0)}$ bonds from a right root to a left root contain all the Q vertices and contains them in the same order; (iv) root 1 is attached to the head of a Θ bond; (v) root $1'$ is attached to the tail of a Θ bond; (vi) every free time point is on a Q and is attached to the head of one Θ bond and the tail of another Θ bond; and (vii) there is a unique forward path of Θ bonds leading from root $1'$ to root 1 that contains all the Θ bonds and all the time points on the Q vertices.

Now we make use of the cluster representation of the Q vertices, eq 2. This equation implies that each Q vertex is equal to a sum of contributions, each consisting of one $Q^{(c)}$ and some additional factors. To define this more precisely, first we define new versions of $Q^{(c)}$ by analogy to eq 18

$$Q^{(c)}_{nm}(1t_1 \ldots nt_n; 1't_{1'} \ldots m't_{m'}) = Q^{(c)}_{nm}(1 \ldots n; 1' \ldots m')\left(\prod_{i=2}^{n}\delta(t_i - t_1)\right)\left(\prod_{j=1}^{m}\delta(t_{j'} - t_1)\right) \quad (22)$$

Then by analogy to eq 19, we define a version of $Q^{(c)}$ that has an additional time argument

$$Q^{(c)}_{nm}(1t_1 \ldots nt_n; t; 1't'_1 \ldots m't'_m) = Q^{(c)}_{nm}(1t_1 \ldots nt_n; 1't'_1 \ldots m't'_m)\delta(t - t_1)$$

We define a new version of a δ vertex, called a $\bar{\delta}$ vertex, that has three points, one of which is a time point. The function associated with $\bar{\delta}$ is

$$\bar{\delta}(1t_1; t; 2t_2) = \delta(1; 2)\delta(t_1 - t_2)\delta(t_1 - t)$$

Finally, we define a Δ_m vertex, that has m time points. The function associated with this vertex is

$$\Delta_1(t_1) = 1$$

$$\Delta_m(t_1 \ldots t_m) = \prod_{i=2}^{m}\delta(t_i - t_1) \text{ for } m \geq 1$$

Then

$$Q_{nm}(1t_1, \ldots nt_n; t; 1't_{1'} \ldots m't_{m'}) = \text{the sum of all topologically different matrix diagrams}$$

with (i) n left roots labeled $(1t_1) \ldots (nt_n)$; (ii) m right roots labeled $(1't_{1'}) \ldots (m't_{m'})$; (iii) one root time point labeled t; and (iv) one $Q^{(c)}$ vertex, zero or more $\bar{\delta}$ vertices, and one Δ vertex; such that (i) the root time point is the time point on the $Q^{(c)}$; and (ii) the Δ is attached to the time point of the $Q^{(c)}$ and the time points of each $\bar{\delta}$.

When this is substituted into the previous series, we get

$$\chi_{nm}(1 \ldots n, t_1; 1' \ldots m', t_2) = \text{the sum of all topologically different connected diagrams}$$

with (i) n left roots labeled $(1, t_1) \ldots (n, t_1)$; (ii) m right roots labeled $(1', t_2) \ldots (m', t_2)$; (iii) free points and free time points; (iv) $\chi^{(0)}$ and Θ bonds; and (v) $Q^{(c)}_{pq}$ vertices for $p, q \geq 1$, an equal number of Δ vertices, and $\bar{\delta}$ vertices; such that (i) each root is attached to a $\chi^{(0)}$ bond; (ii) every free point is attached to a $\chi^{(0)}$ bond and a $Q^{(c)}$ vertex; (iii) for diagrams with one or more $Q^{(c)}$, all forward paths of $\chi^{(0)}$ bonds from a right root to a left root contain all the Q vertices and contain them in the same order; (iv) root 1 is attached to the head of a Θ bond; (v) root $1'$ is attached to the tail of a Θ bond; (vi) every free time point is on a Q and is attached to the head of one Θ bond and the tail of another Θ bond; (vii) there is a unique forward path of Θ bonds leading from root $1'$ to root 1 that contains all the time points on the Q vertices; (viii) the free time point on each $Q^{(c)}$ is attached to one and only one Δ; (ix) each Δ is attached to the time free point of one and only one $Q^{(c)}$ and to the time point of zero or more $\bar{\delta}$ vertices; and (x) the time point of each $\bar{\delta}$ is attached to one and only one Δ.

Consider the free points that are on the $\bar{\delta}$ vertices attached to a specific Δ vertex. Integration over the variables for the two points on a δ gives a result equivalent to removing the δ and replacing the two $\chi^{(0)}$ bonds attached to it by a single $\chi^{(0)}$ bond, and reducing the subscript on the Δ by unity, as in the transition from (*c*) to (*d*) in Figure 4. It can be shown that this replacement does not change the symmetry number or the value of a diagram. (The presence of the forward path of Θ bonds makes the points on any $\bar{\delta}$ vertex attached to a specific Δ distinguishable from the points on any $\bar{\delta}$ attached to a different Δ vertex, thus simplifying the analysis of the symmetry numbers for these diagrams. This is the reason we introduced time points and Θ bonds.) When this replacement is completed for each $\bar{\delta}$, each Δ vertex is attached only to the time free point of a $Q^{(c)}$, and the value of each Δ will be unity. So we may as well remove the Δ vertices from the diagrams

$$\chi_{nm}(1 \ldots n, t_1; 1' \ldots m', t_2) = \text{the sum of all topologically different proper connected matrix diagrams} \quad (23)$$

with (i) n left roots labeled $(1, t_1) \ldots (n, t_1)$; (ii) m right roots labeled $(1', t_2) \ldots (m', t_2)$; (iii) free points and free time points; (iv) $\chi^{(0)}$ and Θ bonds; and (v) $Q^{(c)}_{pq}$ vertices for $p, q \geq 1$; such that (i) each root is attached to a $\chi^{(0)}$ bond; (ii) every free point is attached to a $\chi^{(0)}$ bond and a $Q^{(c)}$ vertex; (iii) root 1 is attached to the head of a Θ bond; (iv) root $1'$ is attached to the tail of a Θ bond; (v) every free time point is on a Q and is attached to the head of one Θ bond and the tail of another Θ bond; and (vi) there is a unique forward path of Θ bonds leading from root $1'$ to root 1 that contains all the time points on the Q vertices.

Consider a diagram in this series having a specific number p of Q vertices and hence $p + 1$ Θ bonds, and imagine removing the Θ bonds. Imagine all $p!$ possible ways of adding the Θ bonds back to the diagram so that restriction vi is satisfied. Each of these ways results in a valid diagram in the series. This leads us to consider the following function:

$$T_{p+2}(t_1; t_1'' \ldots t_p''; t_1') = \text{the sum of all topologically different diagrams} \quad (24)$$

with (i) one time root labeled t_1, one time root labeled t_1', and p time roots labeled t_1'', ..., t_p''; (ii) Θ bonds; such that (i) the time root labeled t_1 is attached to the head of a Θ bond; (ii) the time root labeled t_1' is attached to the tail of a Θ bond; (iii) every other time root is attached to the head of one Θ bond and the tail of another Θ bond; and (iv) there is a forward path of Θ bonds from the root labeled t_1' to the root labeled t_1.

The $p!$ diagrams in this series each correspond to one possible ordering of the time arguments such that t_2 is the earliest and t_1 is the latest. The sum is just equal to

$$T_{p+2}(t_1; t_1'' \ldots t_p''; t_1') = \prod_{j=1}^{p} (\Theta(t_1 - t_j)\Theta(t_j - t_1'))$$

It can be shown, by applying straightforward a generalization of the lemmas of Morita and Hiroike,[11] that the series above for χ_{nm} is equal to a series with the same structure but with Θ bonds replaced by a T vertex attached to all of the time points and to roots 1 and $1'$. This series would be unaffected in value if the T vertex were then removed from each diagram. Whenever T is zero, the rest of the integrand is zero anyway because of the Heaviside time dependence of the $\chi^{(0)}$ bonds. Thus, we remove the T. At this point, the time points on the $Q^{(c)}$ have no effect on the value of the diagram and nothing is attached to them. We remove them and each $Q^{(c)}$ is now of the form that has no time point. We get the result quoted above in eq 5.

References and Notes

(1) Andersen, H. C. *J. Phys. Chem. B* **2002**, *106*, 8326. Referred to as I in the present paper.

(2) Andersen, H. C. *J. Phys. Chem. B* **2003**, *107*, 10226. Referred to as II in the text.

(3) Gross, E. P. *Ann. Phys. (N.Y.)* **1972**, *69*, 42.

(4) Bergeron, K. D.; Gross, E. P.; Varley, R. L. *J. Stat. Phys.* **1974**, *10*, 111.

(5) Gross, E. P. *J. Stat. Phys.* **1976**, *15*, 181.

(6) Boley, C. D. *Phys. Rev.* **1975**, *A11*, 328.

(7) Lindenfeld, M. *Phys. Rev.* **1977**, *A15*, 1801.

(8) Mazenko, G. F. *Phys. Rev.* **1974**, *A9*, 360.

(9) Mazenko, G. F.; Yip, S. In *Statistical Mechanics. Part B: Time-Dependent Processes*; Berne, B. J., Ed.; Plenum: New York, 1977.

(10) Mayer, J. E.; Mayer, M. G. *Statistical Mechanics*; Wiley: New York, 1940.

(11) Morita, T.; Hiroike, K. *Prog. Theor. Phys.* **1961**, *25*, 537.

(12) Stell, G. Cluster Expansions for Classical Systems in Equilibrium. In *The Equilibrium Theory of Classical Fluids*; Frisch, H. L., Lebowitz, J. L., Eds.; W. A. Benjamin: New York, 1964.

(13) Andersen, H. C. Cluster Methods in Equilibrium Statistical Mechanics of Fluids. In *Statistical Mechanics, Part A: Equilibrium Techniques*; Berne, B. J., Ed.; Plenum: New York, 1977; p 1.

(14) Hansen, J.-P.; McDonald, I. R. *Theory of Simple Liquids*, 2nd ed.; Academic: London, 1986.

(15) See Appendix A of I for a summary of the diagrammatic terminology that we use.

(16) Diagrams with the characteristic of having no bond whose removal disconnects the left roots from the right roots are analogous to diagrams in many-body theory that are called 1-particle-irreducible. See, for example: Zinn-Justin, J. *Quantum Field Theory and Critical Phenomena*; Oxford University Press: New York, 1989.

(17) Götze, W. In *Liquids, Freezing and the Glass Transition*; Levesque, D., Hansen, J. P., Zinn-Justin, J., Eds.; North-Holland, New York, 1991; Part I, p 287.

(18) Sjögren, L. *Phys. Rev.* **1980**, *A22*, 2866.

(19) Hugenholtz, N. M. *Physica* **1956**, *22*, 343; reprinted in *Problems in Quantum Theory of Many-Particle Systems*; Van Hove, L., Hugenholtz, N. M., Howland, L. P., Eds.; W. A. Benjamin: New York, 1961.